ISSN 1063-7834, Physics of the Solid State, 2019, Vol. 61, No. 10, pp. 1910–1914. © Pleiades Publishing, Ltd., 2019.
Russian Text © The Author(s), 2019, published in Fizika Tverdogo Tela, 2019, Vol. 61, No. 10, pp. 1948–1952.

PHYSICS OF SURFACE AND THIN FILMS

The Effect of Synthesis Temperature on the Microstructure and Electrophysical Properties of BST 80/20 Films

M. S. Afanas'ev[a], D. A. Kiselev[a, b], S. A. Levashov[a], A. A. Sivov[a], and G. V. Chucheva[a, *]

[a] *Fryazino Branch of Kotelnikov Institute of Radioengineering and Electronics, Russian Academy of Sciences, Fryazino, 141190 Russia*

[b] *National Research Technological University "MISiS", Moscow, 119049 Russia*

**e-mail: gvc@ms.ire.rssi.ru*

Received April 22, 2019; revised April 22, 2019; accepted April 23, 2019

Abstract—In this paper, we show the effect of synthesis temperature on the microstructure and electrophysical properties of ferroelectric $Ba_{0.8}Sr_{0.2}TiO_3$ films during the formation on silicon substrates with a platinum sublayer. Based on our measurements, we conclude that temperature of synthesis of ferroelectric films affects their electrophysical and topographical properties.

Keywords: metal-dielectric-metal structures, $Ba_{0.8}Sr_{0.2}TiO_3$ ferroelectric films, microstructure, electrophysical properties, scanning probe microscopy

DOI: 10.1134/S1063783419100032

1. INTRODUCTION

Prospects for the creation and development of the next generations of information storage and processing devices are associated with the use of new, both in composition and in structure, structural materials. Ferroelectrics are of great interest as a structural material. One of the important areas is the use of ferroelectrics as insulating layers in metal-dielectric-metal (MDM) structures.

Among the ferroelectrics being studied today, the most attractive are oxide materials with a perovskite structure with the general formula ABO_3. An important feature of such substances is the ability to form multicomponent solid solutions that allows creating materials, whose electrophysical properties vary over a wide range. At present, the most promising ferroelectric materials for memory systems and microwave applications are considered to be solid solutions of barium, strontium, and lead zirconates [1–3]. The barium strontium titanate (BST) films should be used in microelectronics as a material with high dielectric constant (high-k) in the transition to topological standards of 90 nm and less [4]. Characteristics of electronic devices, the principle of which is based on the use of BST films, largely depends on the composition and properties of the ferroelectric layer. A change in the component composition of BST films was shown to allow controlling the magnitude of the static dielectric constant, UHF losses, and temperature properties of the film [5]. The results of studies on the effect of the operating gas pressure in ion-plasma sputtering on the properties of deposited ferroelectric coatings of barium strontium titanate are presented in [6]. The variation of the operating gas pressure during deposition of BST films is established to allow changing the component composition of the deposited layer. This leads to a smearing of the phase transition and an improvement in the temperature stability of the ferroelectric film properties [6]. In this work, we study the effect of synthesis temperature on the microstructure and electrophysical properties of $Ba_{0.8}Sr_{0.2}TiO_3$ ferroelectric films.

2. MATERIALS AND EXPERIMENTAL METHODS

For the studies, MDM structures comprising of a silicon substrate with a platinum sublayer, a ferroelectric film of composition $Ba_{0.8}Sr_{0.2}TiO_3$ and an upper nickel electrode were fabricated. A ferroelectric film with a thickness of 450 ± 25 nm was deposited on a platinum electrode by high-frequency sputtering of a polycrystalline target in an oxygen atmosphere using a Plasma-50SE setup (Russia). The setup design and film deposition technique are given in [7, 8]. The substrate temperature during the synthesis was 560 and 620°C. An upper nickel electrode was deposited on the ferroelectric film through a shadow mask by the electron beam using an A700QE/DI12000 setup (Germany). The electrode area was 2.7×10^{-4} cm^2, and the electrode thickness was 0.1 μm. The results of fluoroscopic studies of such samples are presented in [9].

The study of the electrophysical properties of the resulted MDM structures was performed on an auto-

mated measuring stand [10] using a precision LCR meter Agilent E4980A, a portable computer with modified software, and a special camera equipped with a thermostabilized heating table. The effective dielectric permeability of the structure was calculated using the formulas for a flat capacitor based on measurements carried out according to the method described in [11, 12].

The topography of BST films was obtained in contact mode using a scanning probe microscope MFP-3D SA (Asylum Research, USA) together with an Asyelec-02 brand cantilever (Asylum Research, USA). Image processing and analysis were performed using the Gwyddion and WSxM software [13].

3. RESULTS AND DISCUSSION

3.1. Electrophysical Properties

Figure 1 shows the volt-farad characteristics (VF characteristics) of film capacitors based on BST films measured at room temperature at a frequency of 100 kHz. The sample was supplied with a bias voltage V_g of from −16 to +16 V (curves *1* and *3*) and reverse (curves *2* and *4*) with a 0.25-V step and a measuring signal amplitude of 25 mV at a data reading rate of three points in s.

The electric field enhances the anharmonicity of lattice vibrations in a ferroelectric film, leading to a decrease in the value of its dielectric permeability. The maximal capacitance values for Pt/BST/Ni samples were observed at $V_g \approx -1.1$ V for BST films synthesized at 560°C and $V_g \approx -0.4$ V for the films obtained at 620°C. The shift of the maximum with respect to the point $V_g = 0$ V can be caused by the presence of an internal electric field in the ferroelectric film, the appearance of which is associated with differences in the structure and charge state of the lower and upper Pt/BST/Ni interfaces.

BST film-based capacitors synthesized at 620°C are characterized by higher capacitance values compared with similar MIM structures obtained at 560°C. The curves of capacitance versus the bias voltage are bell-shaped. In a sample synthesized at 620°C, the VF characteristics are more pronounced and symmetric about the vertical axis (see Fig. 1, curves *1* and *2*). Besides, the curves describing the change in capacitance with voltage and corresponding to different directions of measurements of the VF characteristic (direct (curve *1*) and reverse (curve *2*)) are more similar to each other precisely for BST film-based capacitors synthesized at 620°C. This suggests a more stable behavior of the structures obtained at 620°C.

The controllability coefficient of the MDM structure calculated as the ratio of capacitances at the minimal and maximal applied field reaches a value of 1.8 for a capacitor based on a BST film synthesized at 560°C and a value of 1.87 for a sample based on a BST film obtained at 620°C. This also suggests a higher controllability of a capacitor based on a film obtained at 620°C.

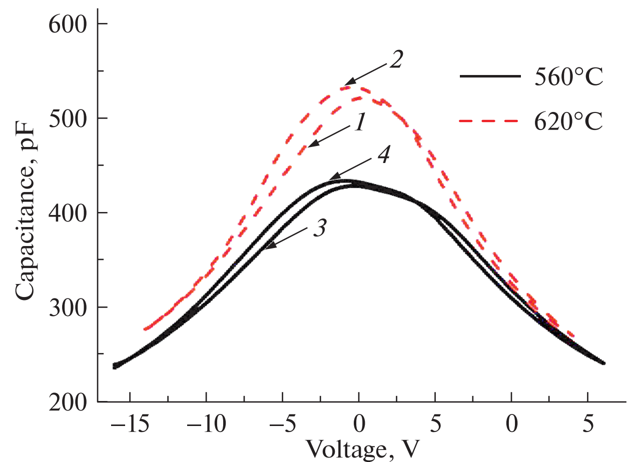

Fig. 1. Dependence of the capacitance of film capacitors based on BST films synthesized at 560°C (curves *3*, *4*) and 620°C (curve *1*, *2*) on the bias voltage V_g at a frequency of 100 kHz and room temperature.

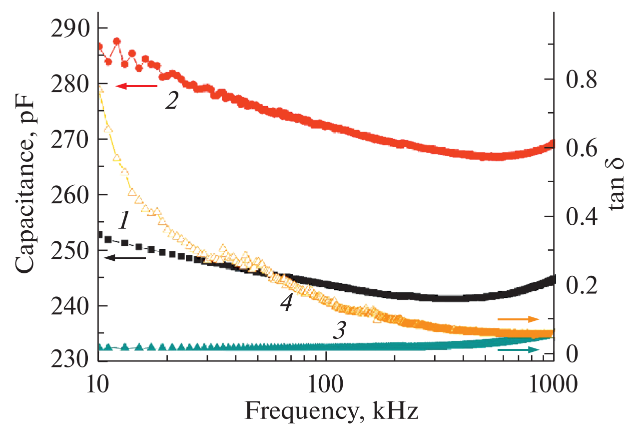

Fig. 2. Frequency dependences of capacitance (curves *1* and *2*) and dielectric loss tangent (curves *3* and *4*) of film capacitors based on BST films synthesized at 560°C (curves *1* and *3*) and 620°C (curves *2* and *4*) measured at a bias voltage of $V_g = 15.0$ V and room temperature.

Figure 2 shows the measured at room temperature and constant bias $V_g = 15.0$ V frequency dependences of the capacitance and the dielectric loss tangent of Pt/BST/Ni capacitors based on BST films and synthesized at 560 and 620°C. As the frequency increases, capacitances for both samples decrease in the frequency range of 10–850 kHz and increase at the frequency above 850 kHz. In this case, Pt/BST/Ni capacitors based on BST films synthesized at 620°C (curve *2*) demonstrate higher capacitance values than those for samples based on BST films obtained at 560°C (curve *1*). The dielectric loss tangent for an

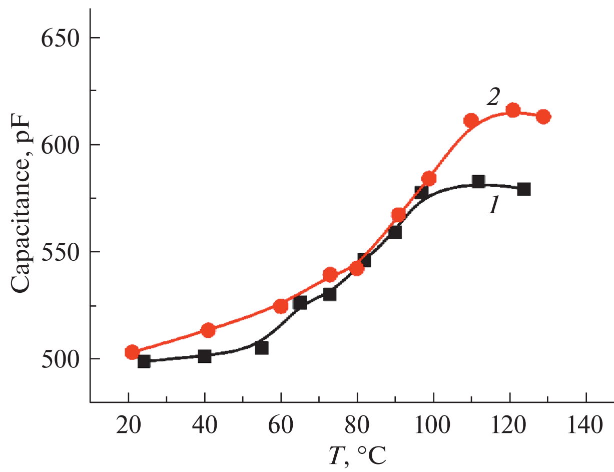

Fig. 3. Temperature dependence of the capacitance of film capacitors based on BST films synthesized at 560°C (curve *1*) and 620°C (curve *2*) measured at a bias voltage of V_g = 0 V and a frequency of 100 kHz.

MDM structure based on a BST film synthesized at 620°C (curve *4*) has a sharp drop with a frequency in the range of 10–500 kHz, then the fall slows down with increasing frequency (the value of the dielectric loss tangent is approximately 0.1) and reaches the minimal value at 1 ± 0.1 MHz. The dielectric loss tangent for this sample drops from 0.75 at 10 kHz to 0.06 at 1 MHz. For samples based on films synthesized at 560°C (curve *3*), the plot of the frequency dependence of the dielectric loss tangent has the form of a straight line parallel to the *X*-axis in the range of 10–500 kHz, passing into a slight increase in the range of 500–1000 kHz. The value of the dielectric loss tangent is 0.02 in the frequency range of 10–500 kHz and increases to a value of 0.06 in the range of 500–1000 kHz.

Figure 3 shows the temperature dependences of the capacitance of film capacitors based on BST films at a zero bias voltage and a frequency of 100 kHz. The measurements were performed in the temperature range from 20 to 130°C. At an increase in temperature, an increase in the capacitance (respectively, and an increase in the dielectric permittivity) of the structure is observed, and a part of the dependence in the temperature range of 70–100°C is characterized by the most rapid increase in values. Starting with a temperature of 110°C, the capacity growth almost ceases, and changes in the values lie within the measuring error while a confident decrease in the capacitance is observed starting from 120°C. The capacitance values for the sample based on the BST film synthesized at 620°C (curve *2*) are higher than those for the MDM structure based on the BST film obtained at 560°C (curve *1*). The maximal value of capacitance in MDM structures was observed at a temperature of $T \approx 120$°C.

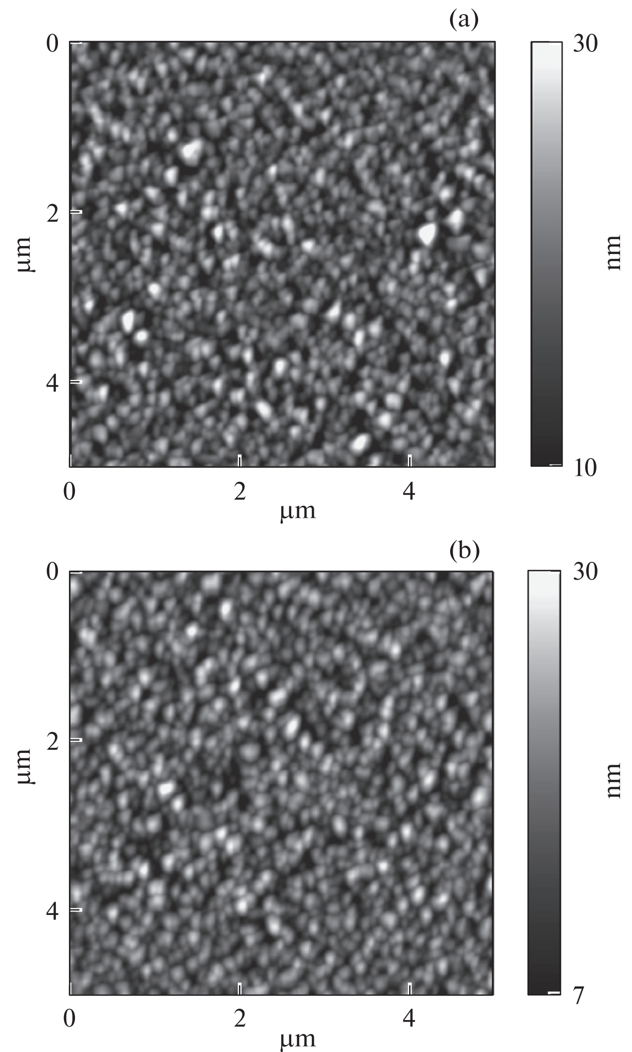

Fig. 4. Surface images of BST films obtained at various synthesis temperatures ((a) 560°C and (b) 620°C).

3.2. Scanning Probe Microscopy

Figure 4 shows the images of the topography of BST films synthesized at 560 and 620°C. A statistical analysis showed that the mean-square surface roughness (*Rms*) was 4.8 nm for a BST film synthesized at 560°C and *Rms* = 4.7 nm for a BST film synthesized at 620°C. As can be seen in the obtained topographic images, the films are formed from crystallites (grains). To quantify the grain size (correlation length, ξ), we used the autocorrelation function [14], which has the following form:

$$C(r_1, r_2) = \Sigma_{x,y} f(x, y) f(x + r_1, y + r_2), \quad (1)$$

where $f(x, y)$ is the image matrix (in our case, topography images of the film surface). Equation (1) shows the initial image and the offset image at a distance r_1 and r_2 along the *X* and *Y* axes relative to the image center. The resulting image $C(r_1, r_2)$ is a measure of how

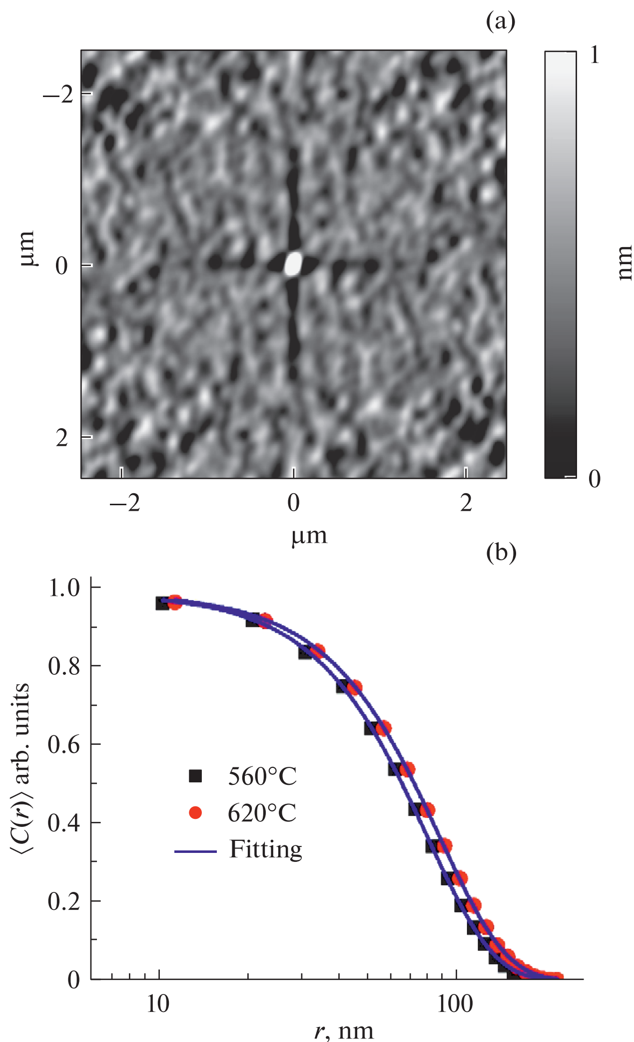

Fig. 5. (a) 2D-representation of the autocorrelation function obtained from the topographic image of the BST film surface (620°C), and (b) the graph shows the profiles of the autocorrelation function (points) and their approximation by equation (2) (lines) for the BST films under study.

different these two images are. The more similar the initial image and the offset image, the higher the autocorrelation value. Any periodicity in the initial image will represent a periodic pattern in the autocorrelation image. As an example, Fig. 5a shows a 2D representation of the autocorrelation function for a BST film synthesized at 620°C. Furthermore, by extracting a plot of the radially averaged values of the desired parameter from the obtained auto-correlation image, the average grain size can be determined by the scanned surface area of the BST film. For this purpose, the equation of the following form is used [14]:

$$\langle C(r)\rangle = A\exp[-(r/\langle\xi\rangle)^{2h}], \quad (2)$$

where A is the constant, r is the distance from the central peak (nm) determined from the autocorrelation function image, ξ is the average grain size (nm), and h ($0 < h < 1$) is the parameter.

Figure 5b shows the approximated dependences of the correlation function for determining the average grain size in the films under study. Calculations showed that the average grain size was 78 nm for BST films synthesized at 560°C and ξ = 87 nm for BST films synthesized at 620°C. Thus, the synthesis temperature affects the grain size in BST films, which, in turn, leads to an increase in the dielectric characteristics.

4. CONCLUSIONS

Performed studies indicated the effect of the synthesis temperature of thin BST films on the dielectric characteristics of BST-based MIM-structures. The samples synthesized at a temperature of 620°C were found to have higher values of capacitance (and, accordingly, dielectric permittivity) and controllability compared with the structures obtained at 560°C. An increase in the synthesis temperature also leads to an increase in the average grain size in the ferroelectric film.

FUNDING

This work was performed within the framework of a state assignment and was partially supported by the Russian Foundation for Basic Research, projects nos. 18-29-11029 and 19-07-00271. Scanning probe microscopy studies were partially supported by the Ministry of Science and Higher Education of the Russian Federation, project no. 11.9706.2017/7.8.

CONFLICT OF INTEREST

The authors declare that they have no conflicts of interest.

REFERENCES

1. K. A. Vorotilov, V. M. Mukhortov, and A. S. Sigov, *Integrated Ferroelectric Devices*, Ed. by A. S. Sigov (Energoatomizdat, Moscow, 2011) [in Russian].
2. A. K. Tagantsev, V. O. Sherman, K. F. Astafiev, J. Venkatesh, and N. Setter, J. Electroceram. **11**, 5 (2003).
3. K. M. Rabe, Ch. H. Ahn, and J.-M. Triscone, *Physics of Ferroelectrics: A Modern Perspective*, Topics in Applied Physics (Springer, Berlin, Heidelberg, 2007).
4. S. Ezhilvalavan and Tseung-Yuen Tseng, Mater. Chem. Phys. **65**, 227 (2000).
5. A. V. Tumarkin, E. R. Tepina, E. A. Nenasheva, N. F. Kartenko, and A. B. Kozyrev, Tech. Phys. **57**, 787 (2012).
6. A. V. Tumarkin, S. V. Razumov, V. A. Volpyas, A. G. Gagarin, A. A. Odinets, M. V. Zlygostov, and E. N. Sapego, Tech. Phys. **62**, 1592 (2017).

7. M. S. Afanas'ev and M. S. Ivanov, Phys. Solid State **51**, 1328 (2009).
8. D. A. Kiselev, M. S. Afanasiev, S. A. Levashov, and G. V. Chucheva, Phys. Solid State **57**, 1151 (2015).
9. M. S. Afanasiev, D. A. Kiselev, S. A. Levashov, V. A. Luzanov, A. E. Nabiev, V. G. Naryshkina, A. A. Sivov, and G. V. Chucheva, Phys. Solid State **60**, 954 (2018).
10. E. I. Gol'dman, A. G. Zhdan, and G. V. Chucheva, Instrum. Exp. Tech. **40**, 841 (1997).
11. T. Hamano, D. J. Towner, and B. W. Wessels, Appl. Phys. Lett. **83**, 5274 (2003).
12. P. M. Suherman, T. J. Jackson, Y. Y. Tse, I. P. Jones, R. I. Chakalova, M. J. Lancaster, and A. Porch, J. Appl. Phys. **99**, 104101 (2006).
13. I. Horcas, R. Fernández, J. M. Gomez-Rodriguez, J. W. S. X. Colchero, J. W. S. X. M. Gómez-Herrero, and A. M. Baro, Rev. Sci. Instrum. **78**, 013705 (2007).
14. R. C. Munoz, G. Vidal, M. Mulsow, J. G. Lisoni, C. Arenas, A. Concha, and R. Esparza, Phys. Rev. B **62**, 4686 (2000).

SPELL: OK